

Energy Efficiency Testing and Power Modeling of O-RAN Radio Units

Zhuohuan Li, Prasanthi Maddala,
N. K. Shankaranarayanan, Ivan Seskar
Rutgers University, WINLAB,
New Jersey, USA

Sarat Puthenpura, Alexandru Stancu
Open Networking Foundation,
California, USA

Christian Nunez Alvarez,
Gregg Albrecht
Keysight Technologies,
California, USA

Abstract— The power consumption of O-RAN Radio Units (O-RUs) is a dominant factor in the overall energy efficiency and sustainability of O-RAN networks. To develop effective energy management solutions, detailed O-RU energy tests and accurate power consumption models are essential. This paper presents a comprehensive study on multi-vendor O-RU energy efficiency, making two key contributions: (a) we introduce a versatile O-RU energy testing platform and present a comprehensive set of power measurements from multiple O-RUs across various operational parameters, including MIMO configurations and traffic loads; (b) we leverage this empirical data to parameterize and validate a component-based power model. Our findings provide critical insights into O-RU power dynamics, enabling the refinement of energy-saving algorithms and supporting the sustainable evolution of O-RAN deployments.

Index Terms—O-RAN, Energy Efficiency, Energy Testing, Power Modeling, KPI Optimization

I. INTRODUCTION

Fifth-generation (5G) wireless communication is a transformative technology that promises to revolutionize various industry sectors. With the densification of base stations and the use of advanced antenna technologies like Multiple-Input Multiple-Output (MIMO), the energy demand of 5G networks has become a critical concern. An important part of the 5G network evolution is the concept of Open Radio Access Network (O-RAN), an open, disaggregated, and software-defined architecture that enables multi-vendor interoperability, flexible network deployments, and integration of artificial intelligence (AI) for dynamic network management. However, despite these benefits, the energy consumption of O-RAN-based 5G networks remains a crucial issue due to the increased complexity and additional operational requirements introduced by the disaggregation of network functions. Energy efficiency has emerged as a critical Key Performance Indicator (KPI) for next-generation RAN architectures [1]. Projections indicate that if current practices persist, the global energy consumption of mobile networks could account for up to 20% of the world's total electricity usage by 2030, with approximately 80% of this consumption attributed to widely distributed base stations [2]. This scenario poses a substantial threat to the sustainability of wireless networks, underscoring the urgent need for innovative energy-saving solutions.

In a previous paper [3], we presented the objectives of our research program on O-RAN energy efficiency. In this

work, we focus on the O-RU, whose power consumption is a dominant factor for sustainability due to the large number of deployed units. The global deployment of 5G O-RAN architectures presents an energy efficiency paradox: while the disaggregated architecture with O-RUs enhances network flexibility and promotes multi-vendor interoperability, the lack of standardized energy efficiency metrics across heterogeneous O-RUs adds to the complexity of power management.

Energy efficiency in O-RAN is influenced by various factors, including hardware technology efficiency, optimization of radio access network (RAN) resources, and the intelligent management of network traffic. A key opportunity in O-RAN energy optimization lies in reducing the power consumption of O-RUs while maintaining high-quality service levels. Several state-of-the-art, energy-saving techniques have been proposed, including symbol, channel, and carrier shutdown [4], as well as RF reconfiguration. Among the most promising of these are Advanced Sleep Modes (ASMs), a technique for 5G base stations that progressively deactivates different RAN components to achieve various sleep depths [5]. However, despite the potential of these methods, their practical implementation in multi-vendor O-RAN systems is still in its early stages and requires significant refinement to meet the demanding requirements of 5G networks [7]. Given the dominance of O-RU power consumption and that energy optimization has multiple dimensions, it is critical to have a good methodology for O-RU energy testing, and also a good power consumption prediction model to be used in network optimization when resources can be scaled back and devices can be turned off to save energy.

While there have been studies and models of power consumption of O-RUs and pre-O-RAN base stations [2]–[6], there are very few detailed measurements available in the literature. We have found papers with different models and equations for O-RU power consumption without all the supporting measured data. In this paper, we present our methodology and detailed results of O-RU energy efficiency tests and also propose a power model consistent with our measurements. We hope this contribution benefits fellow researchers in need of similar data and facilitates further advancements in the field.

The remainder of this paper is structured as follows: Section II introduces our component-based power model. In Section III, we describe our O-RU energy testing platform. In Section IV we analyze the measurement data, present the parameterized models, and discuss the key findings on

power consumption dynamics. Finally, Section V summarizes our contributions and discusses potential direction for future research.

II. O-RU POWER MODELING

O-RU power modeling is a key aspect of O-RAN energy efficiency optimization. The establishment of an accurate power consumption model is crucial for development and evaluation of advanced energy-saving strategies. In the context of a functional split 7.2x O-RU architecture, prior work, such as Usman et al. [5], has established component-based analytical models that offer valuable physical insights by distinguishing between digital and analog components. The primary challenge for such models, however, lies in accurately parameterizing their non-linear, multi-dimensional components with real-world hardware data. Addressing this challenge, our study implements and parameterizes a similar, widely recognized analytical framework for various O-RU categories. Previous studies have reported that the O-RU power consumption increases as the RF power output from the PA increases, and at high powers, this is dominated by the efficiency of the PA [9]. The power consumption also increases as the number of antenna chains increase, and also as the O-RU utilization (e.g., the downlink PRB utilization) increases. Our study provides insights into how these inter-related factors can be combined into a model.

To accurately evaluate the energy efficiency of the network, we build on a widely-recognized power consumption modeling approach for the O-RU [10], based on the specifications from the O-RAN Alliance and related academic research. The total power consumption, P_{O-RU} , is formulated as:

$$P_{O-RU} = P_{base} + N_{TX} \left(P_{idle-ch} + \frac{P_{tx-ch}(\mu)}{\eta_{PA}(P_{tx-ch})} + \alpha_{O-RU}(\mu) \right) \quad (1)$$

where the parameters are defined as follows:

- P_{base} : The static baseline power consumption of the O-RU, representing the power drawn by components such as the power supply, and baseband processor in an idle (no RF transmission) state.
- N_{TX} : The number of active transmit (Tx) antenna chains.
- $P_{idle-ch}$: The power consumed by a single RF chain when it is idle (active but not transmitting RF power). This power is dependent on the operational bandwidth B .
- μ : The resource utilization factor ($0 \leq \mu \leq 1$), or load, corresponding to the fraction of Physical Resource Blocks (PRBs) being used for downlink transmission
- P_{tx-ch} : The radio frequency (RF) output power at the antenna port for a single chain.
- $\eta_{PA}(P_{tx-ch})$: The efficiency of the PA, which is a non-linear function of its output power, P_{tx-ch}
- α_{O-RU} : The additional power overhead for digital signal processing and RF circuitry, which scales with the transmission load and system bandwidth.

The model in Eq. (1) captures the key aspects of O-RU power consumption. It deconstructs the total power draw into

a baseline idle power, idle RF chain power and a load-dependent dynamic portion, assuming all chains are identical. This dynamic component is primarily driven by the PA, whose consumption is inversely proportional to its non-linear efficiency η_{PA} . Characterizing this efficiency is a key focus of our work, as it is one of the most critical parameters in our model.

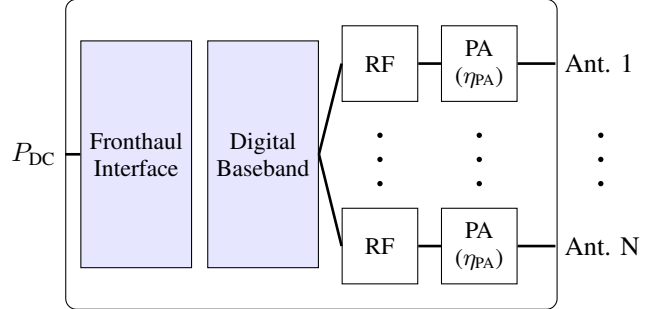


Figure 1. Block Diagram of a MIMO O-RU

The block diagram in Fig. 1 provides a physical basis for our power model by illustrating the architecture of a typical MIMO O-RU. The total DC input power P_{DC} is consumed by several key hardware stages that directly map to our model's components. The Fronthaul Interface and Digital Baseband blocks constitute the static baseline power P_{base} . The signal is then split into parallel RF chains, where each chain's RF block corresponds to the semi-static power $P_{idle-ch}$. Finally, the PA in each chain is the primary factor in the dynamic power, governed by its efficiency η_{PA} . This architectural framework provides the foundation for the parameterization presented in Section IV.

For an O-RU, we can define an Energy Efficiency KPI:

$$EE_{O-RU} = \frac{\text{Total Tx RF Power}}{\text{Power Consumed by O-RU}} \quad (2)$$

The total RF power is proportional to the information delivery capability, and can be directly measured at the O-RU. Having established the analytical frameworks for O-RU power consumption, we now turn to the empirical methodology used to validate them. Our key contribution is the test methodology and the validation and parameterization of the above model, where we extract these crucial values from targeted laboratory measurements. The following section details our experimental setup designed for precise and repeatable energy efficiency measurements under a wide range of operational conditions.

III. EXPERIMENTAL SETUP

A. O-RU Categories

In this study, we evaluate four commercial O-RUs selected to represent a range of deployment scenarios. The detailed specifications for each O-RU are provided in Table I. Our tests cover low RF power (O-RU A), medium RF power (O-RU B), and high RF power (O-RUs C and D). O-RUs A, B, C have 4 antennas while O-RU D has 8 antennas. O-RUs A, B, D

Table I
COMPARATIVE SPECIFICATIONS OF O-RU CATEGORIES

| O-RU | Category (Single RF Chain Max Power) | Duplex / Bandwidth (MHz) | O-RU Power (W) | Antenna |
|--------|--------------------------------------|--------------------------|----------------|------------|
| O-RU A | Low Power (24 dBm) | TDD / 100 | 38-51 | 4 antennas |
| O-RU B | Medium Power (37 dBm) | TDD / 100 | 42-110 | 4 antennas |
| O-RU C | High Power (47 dBm) | FDD / 10 | 192-531 | 4 antennas |
| O-RU D | High Power (47 dBm) | TDD / 100 | 230-800 | 8 antennas |

are TDD (100 MHz, 3.6 GHz), while O-RU C is FDD (10 MHz, 1.8 GHz). O-RU C and D are of a similar high-power design from the same vendor. The table includes the range of measured O-RU power consumption values.

A key aspect of our methodology is the instrumentation used for power measurement. We used managed Power Distribution Units (PDUs) to measure power consumption for all O-RUs and other components. The PDUs are suitable for monitoring all units. They measure total unit AC power and thus represent the full power which is relevant for energy costs and environmental impacts. To achieve higher precision than PDUs and facilitate automated energy tests, we also used a high-precision Keysight DC Power Supply (DCPS) for O-RU B for the automated experiments. Our results allow comparison of the two power measurements and the impact of the AC power adapter in the PDU measurements.

B. O-RU Energy Testing Platform

Our experimental platform, shown in Fig. 2, is designed for a comprehensive evaluation of O-RU energy efficiency and performance within an O-RAN compliant architecture. The core components include a Keysight S5040A O-DU Emulator with an integrated Vector Signal Analyzer (VSA), an Ethernet switch with Precision Time Protocol (PTP) Grand Master (GM) capabilities, the O-RU(s) under test, an RF power meter, the Keysight DCPS, the PDUs, as well as a data logging/viewing system. The PDU and DCPS power consumption measurements are logged in a database.

The O-DU Emulator generates standard-compliant Open Fronthaul (OFH) downlink (DL) signals, which are sent to the O-RU through the Ethernet switch. The O-RU processes the DL frames and transmits at the DL carrier frequency. The RF output is captured by the VSA to validate the signal and make measurements. An RF power meter was used to measure total RF power and used to calibrate the VSA power measurement. This setup allows tests with different MIMO modes, and full/partial loading of the DL frames. The platform can be operated manually (manually configured DL signals), or via an automated test suite that implements ETSI-defined Static Energy Test load scenarios (e.g., Full, Busy, Medium, Low) [7].

Overall, this testbed enables a holistic and repeatable assessment of O-RU power consumption as a function of its key operational parameters, supporting advanced research in disaggregated RAN architectures.

IV. EXPERIMENTAL RESULTS AND MODEL VALIDATION

Our objective is to establish an O-RU energy testing methodology, collect a comprehensive dataset of power measurements, and leverage this data to validate the O-RU power consumption model proposed in Section II.

Figure 3 shows the measured O-RU power consumption as a function of the total RF output power for the four O-RUs. The y-axis uses a logarithmic scale to capture the wide range of power consumption values, while the x-axis is presented in dBm. The measurements show the power operation ranges of the O-RUs. The power consumption increase with RF power is negligible for the low-power O-RU A, and most pronounced for the high-power O-RUs C and D. For O-RU B, the figure has both PDU and DCPS power measurements showing a difference of about 20W due to AC adapter overhead. Based on Eq. (2), for PDU based power, the maximum energy efficiency of O-RUs A, B, C, and D are approximately 1%, 4.4%, 15.7%, and 19.0% respectively, highlighting a substantial disparity across power classes.

The next subsection leverages measurements to parameterize and validate the proposed component-based power model.

A. Model Parameterization and Power Amplifier Efficiency

With the component-based model from Eq. (1) as our framework, we now use our empirical data to determine its key parameters. Our measurements confirm the model's structure, revealing distinct behaviors in different operational regions that align with the model's physical assumptions.

We will now focus on the High-Power O-RU C to understand and measure the impact of MIMO configuration. The results are illustrated in Fig. 4, which plots the O-RU C PDU power consumption against the total RF output power for 1-antenna, 2-antenna, and 4-antenna configurations at full downlink utilization. As expected, the power consumption increases as the total RF power increases. Note that the curves are very close for the three MIMO configurations, thus showing the total RF power as a primary factor driving the power consumption. The plot reveals two key behaviors consistent with our component-based model (Eq. (1)). For any given RF output power, the total O-RU power consumption is slightly higher with the number of active antenna chains. This is attributed to the added idle power of each RF chain $P_{\text{idle-ch}}$, about 1.67 W in this case. Second, the relationship between consumed power and RF power is distinctly non-linear in the low-power region, as highlighted in the magnified view of Fig. 4, but exhibits a strong linear trend at higher power. Our component-based model provides a clear physical explanation

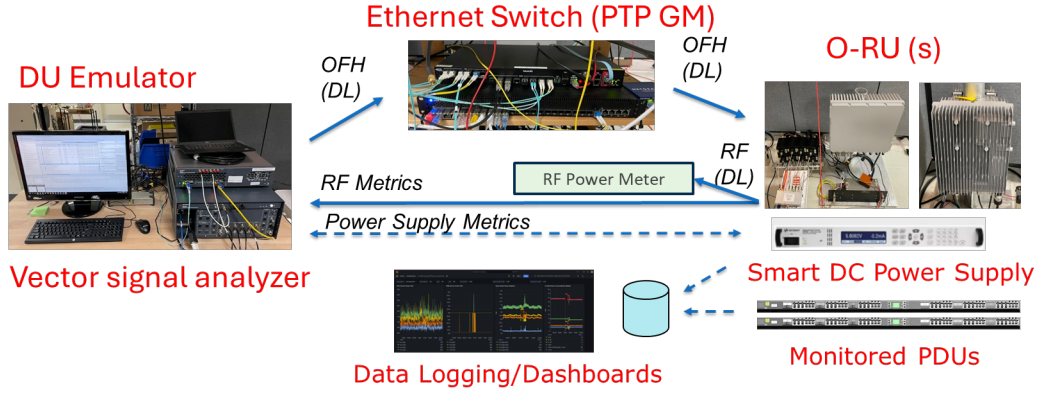


Figure 2. O-DU Emulator based O-RU Energy Testing Platform

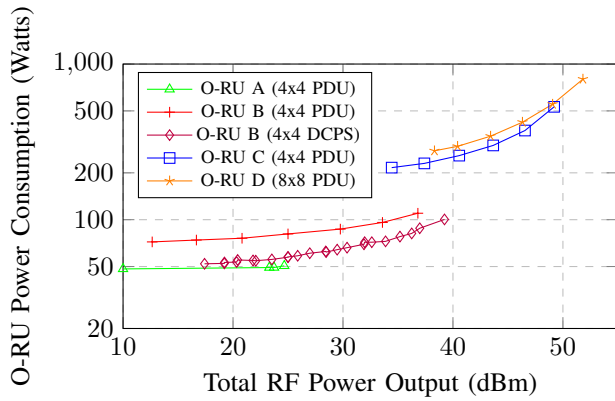


Figure 3. O-RU power consumption (W, log scale) vs. Total RF power output (dBm) for O-RUs A,B,D (PDU) and O-RU B (PDU and DCPS)

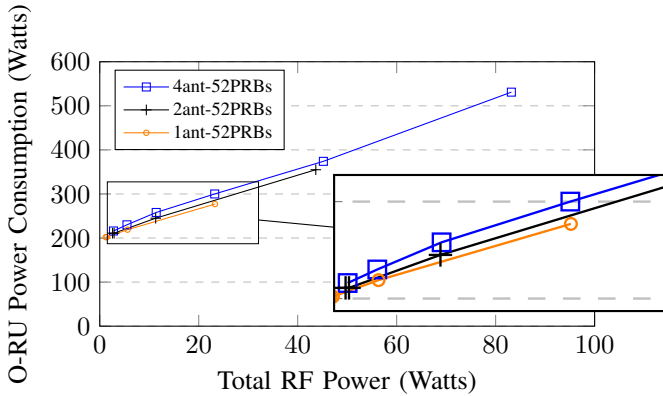


Figure 4. Power consumption vs. Total RF Power for O-RU C for 1x1, 2x2, 4x4 MIMO configurations and full 52-PRB load (10 MHz chbw)

for this behavior. At low power, the non-linearity is driven by rapidly changing PA efficiency ($\eta_{PA}(P_{tx-ch})$). As RF power increases, the PA efficiency saturates, causing the $1/\eta_{PA}(P_{tx-ch})$ term in our model to approach a constant, which produces the observed linear trend. These results show that our component-based model, incorporating PA dynamics, accurately captures the interplay between hardware characteristics and MIMO configurations.

We will now parametrize the model and study the PA efficiency for medium/high power O-RUs B, C, and D. O-RU C and D are of a similar high-power design. Our model (Eq. (1)) has two major parts: a idle part, representing the power consumed at idle operation with no downlink transmission, and a dynamic part, which depends on the total RF output and the PA efficiency, η_{PA} . The idle power can be expressed as

$$P_{idle} = P_{base} + N_{TX} \cdot P_{idle-ch} \quad (3)$$

To estimate the PA efficiency from our measurements, we assume the PA efficiency is the same for all the chains, and also assume the digital signal processing overhead is negligible ($\alpha_{O-RU} \approx 0$) since the PA power consumption is a dominant factor. Then we can isolate the PA efficiency by subtracting the pre-determined idle power (P_{idle}) from the total O-RU power draw (P_{O-RU}), as follows:

$$\eta_{PA} \approx \frac{P_{out}}{P_{O-RU} - P_{idle}} = \frac{N_{TX} \cdot P_{tx-ch}}{P_{O-RU} - P_{idle}} \quad (4)$$

where P_{out} is the total measured RF output power.

We used PDUs to measure the power consumption for all O-RUs. For O-RU B, we also compared the use of PDU and DCPS to measure the power consumption. For O-RU C, the measured idle PDU power consumption values were 192 W (1-layer) and 197 W (4-layer). For O-RU D, the PDU value was 230 W (4-layer). For O-RU B, the PDU values at idle were 42 W for 2-layer MIMO and 46 W for 4-layer MIMO. For O-RU B, the DCPS value at idle was 66 W for 4-layer MIMO. We expect this to be an additive 20 W extra. From these measurements, we derive P_{base} as 38 W for O-RU B and 190.3 W for O-RU C, while $P_{idle-ch}$ is estimated as 2 W and 1.67 W for O-RU B and O-RU C, respectively.

Fig. 5 shows the calculated results of PA Efficiency versus the RF Tx power per chain (Total RF Power/ N_{TX}) for O-RUs B, C, and D. As the plot shows, the efficiency of all units is highly non-linear and dependent on the operational power level, which is a key finding of our study. For all configurations, efficiency is markedly low at low output power (e.g., often below 15% for per-antenna RF outputs under 2.5 W) and

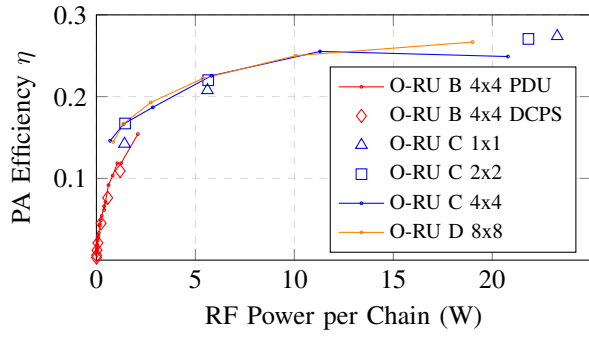


Figure 5. PA efficiency η vs. RF Tx Power per chain for O-RU B (4x4 MIMO, PDU and DCPS), O-RU C (1x1, 2x2, 4x4 MIMO) and O-RU D (8x8 MIMO)

Table II

O-RU B DCPS POWER CONSUMPTION (AND TOTAL RF POWER) (W) vs. LOAD (ETSI STATIC TEST SPEC) FOR DIFFERENT TX.GAIN

| Tx.Gain (dBm) | Low Load | Medium Load | Busy Load | Full Load |
|---------------|--------------|--------------|--------------|---------------|
| 21.5 | 52.0 (0.055) | 52.3 (0.083) | 53.4 (0.108) | 55.1 (0.110) |
| 24.5 | 53.1 (0.084) | 54.7 (0.152) | 55.6 (0.225) | 58.6 (0.387) |
| 27.5 | 54.5 (0.161) | 57.6 (0.317) | 60.9 (0.499) | 64.2 (0.884) |
| 30.5 | 57.4 (0.316) | 62.5 (0.697) | 66.1 (1.089) | 71.7 (1.830) |
| 33.5 | 62.0 (0.703) | 69.5 (1.551) | 72.6 (2.440) | 81.6 (4.217) |
| 36.5 | 71.7 (1.573) | 77.9 (3.297) | 88.1 (4.991) | 100.4 (8.383) |

improves significantly before exhibiting saturation behavior at higher power regions. The performance of the high-power O-RU C (FDD) and D (TDD), which achieve a peak efficiency of approximately 28%, likely reflects an advanced hardware design optimized for high-power operation. Note that the PA efficiency is per amplifier and thus very similar for O-RU C (4x4) and O-RU D (8x8). In contrast, the Mid-Power O-RU B, which peaks at a lower efficiency of around 15%, may be designed with different priorities, not strictly optimized for power efficiency in this operational range. The plot for O-RU B is also shown for power consumption measured with the DCPS which does not include the AC adapter overhead in the PDU measurement. Note that the effect of an additive overhead is removed in Eq. (4) thus explaining the fact that the the O-RU B PA efficiency estimate is the same with the PDU and the DCPS measurements. The plots for O-RU C reveals subtle variations in calculated PA efficiency across the 1x1, 2x2, and 4x4 MIMO configurations, suggesting that each PA's efficiency is not entirely independent. Factors such as the overall thermal load, which increases with more active chains, and potential coupling between RF components can slightly alter the PA's operating conditions, leading to small differences in efficiency. Understanding these empirically derived curves, along with their measurement context and hardware dependencies, is essential for the accurate application of our power model.

B. Impact of Operational Parameters

To analyze the impact of key operational parameters, we used automated Keysight O-DU Emulator test scripts and the Smart

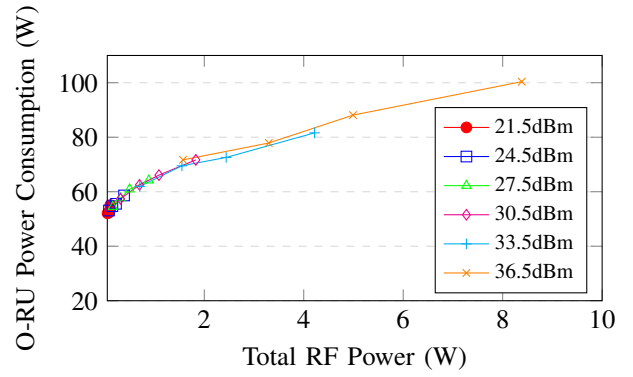


Figure 6. O-RU B Power Consumption vs. Total RF Power for different Tx Gain value (4x4 MIMO)

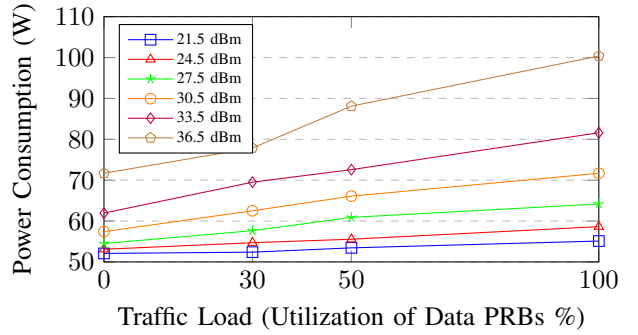


Figure 7. O-RU B Power Consumption vs. Traffic Load corresponding to Low, Medium, Busy, Full load based on ETSI Static Test specs, for different Tx Gain settings

DCPS, and systematically varied two variables: (1) Transmitter Gain, evaluated at six levels from 21.5 dBm to 36.5 dBm in 3 dB increments, and (2) Traffic Load, evaluated at the four ETSI-defined load/utilization levels: Low (0% data, signal PRB), Medium (30%), Busy (50%), and Full (100%) [7]. The loading done in the frequency domain using PRB allocations. This dataset in Table II provides two critical perspectives on O-RU power behavior.

First, we examine the relationship between DC power consumption and the RF Tx power, as shown in Fig. 6. A key finding is that regardless of the specific gain or load setting applied, all data points collapse onto a single, consistent curve. This strongly validates a core assumption of our component-based model (Eq. (1)): the final RF output power is the

Table III
O-RU B DCPS POWER AND RF POWER WITH FREQUENCY VS. TIME DOMAIN

| Load | O-RU Power (W) | | Total RF Power (W) | |
|-------------|----------------|-------|--------------------|------|
| | Freq. | Time | Freq. | Time |
| Low (0%) | 61.57 | 62.36 | 0.65 | 0.63 |
| Med (30%) | 69.16 | 80.67 | 1.55 | 4.14 |
| Busy (50%) | 74.23 | 81.77 | 2.49 | 4.06 |
| Full (100%) | 81.13 | 82.51 | 4.25 | 4.14 |

dominant physical driver of dynamic power consumption. Changes in the internal gain setting and the load values cause a change in the power consumption only when they also change the RF output power.

Second, we analyze the data from an operator’s perspective by plotting DC power against traffic load for each gain setting, as shown in Fig. 7. This view reveals two critical trends consistent with our model. For any fixed gain setting, power consumption increases linearly with traffic load. However, both the power at Low load and the slope of the line are highly dependent on the chosen gain setting. A higher gain results in a higher initial power draw and a steeper increase as load is applied, because it affects the PA’s operating point and overall efficiency (η_{PA}). This provides a view of the operational trade-off for a change in PRB utilization, but the underlying driver is the change in the RF Tx power output as discussed above.

A critical insight from this analysis is the idle power component, which is dominant at low RF power values. For instance, O-RU B consumes about 59 W in an active-idle state (0% utilization). The total DC power increases slightly to 65 W to generate just 1 W of RF output. In this scenario, the idle power constitutes the vast majority—approximately 91%—of the total energy draw. This behavior contrasts sharply with the High-Power O-RU C, where at an 83 W RF output, its idle power of 197 W accounts for a much smaller fraction (37%) of the total 531 W consumption.

C. Impact of Load Generation Method on Power Consumption

Finally, we investigated how the method of generating partial traffic load impacts power consumption. For this, we used the feature in the Keysight DU-Emulator automation script which can generate DL signals for the ETSI Static Energy load levels [7] using a frequency method or a time method. The results in the previous subsection used the frequency-domain approach, where the number of active PRBs is reduced for smaller loads. In the time-domain approach, the number of active transmission slots is reduced for smaller loads. We compare the two methods for the 33.5 dBm fixed gain setting, and the results are shown in Table III.

The load generation method has a profound impact on both the measured RF power and the total power consumption. In the frequency-domain case, the RF power scales proportionally with the number of active PRBs, with a proportionate change in power consumption. However, in the time-domain case, the RF power (and consequently the DC power) increases sharply from Low to Medium load and then changes very little for Medium and Full loads. This suggests that the O-RU may be transmitting at a consistently high power. It is important to note that energy savings features such as DTX, ASM would change this behavior and reduce the power consumption as the load is reduced [5].

This analysis provides an important insight: the effect of utilization on the O-RU power consumption depends on whether the partial loading is achieved by allocating resources in frequency or in time, and also depends on the energy-saving features supported by the O-RU and O-DU.

V. CONCLUSION AND FUTURE WORK

This paper addresses the critical challenge of testing and modeling the power consumption of O-RUs. Our primary contributions are detailed, multi-vendor O-RU power measurements, which are not available in the open literature, and the parameterization and validation of a component-based power model that accurately reflects the underlying hardware behavior. We studied the changes in RU power consumption due to RF power, MIMO layers, transmitter gain, and partial loading (both frequency and time methods). Our analysis revealed the dominance of idle power in low-RF-power scenarios and quantified key performance metrics like PA efficiency. These models and insights provide an essential foundation for developing and deploying the energy-saving algorithms crucial for sustainable O-RAN networks.

Future work will focus on extending the dataset to include measurements from the NTIA-funded ORCID T&E Lab using commercial O-DUs supporting multiple multi-band O-RUs in scenarios replicating a field-deployed operational system. We also hope to refine the model and use them in simulators to explore machine learning for real-time optimization.

ACKNOWLEDGMENT

The authors acknowledge the use of Google Gemini for assistance with minor grammar and style enhancements during the writing process.

REFERENCES

- [1] NGMN Alliance, “Network Energy Efficiency - Phase 2”, October 2023. [Online]. Available: <https://www.ngmn.org/publications/network-energy-efficiency-phase-2.html>
- [2] Andrae AS, Edler T. On global electricity usage of communication technology: trends to 2030. *Challenges*. 2015 Jun;6(1):117-57.
- [3] N. K. Shankaranarayanan et al., “POET: A Platform for O-RAN Energy Efficiency Testing,” 2024 IEEE 100th Vehicular Technology Conference (VTC2024-Fall), Washington, DC, USA, 2024, pp. 1-5, doi: 10.1109/VTC2024-Fall63153.2024.10757537.
- [4] D. López-Pérez et al., “A Survey on 5G Radio Access Network Energy Efficiency: Massive MIMO, Lean Carrier Design, Sleep Modes, and Machine Learning,” in *IEEE Communications Surveys & Tutorials*, vol. 24, no. 1, pp. 653-697, Firstquarter 2022, doi: 10.1109/COMST.2022.3142532.
- [5] M. Q. Usman, C. J. Sreenan, M. Dryjanski and A. O’Driscoll, “Power Modeling of the O-RAN O-RU & Application of Advanced Sleep Modes for Enhanced Energy Efficiency,” 2025 IEEE 22nd Consumer Communications & Networking Conference (CCNC), Las Vegas, NV, USA, 2025, pp. 1-8.
- [6] Salahdine, Fatima, et al. “A survey on sleep mode techniques for ultradense networks in 5G and beyond.” *Computer Networks* 201 (2021): 108567.
- [7] ETSI ES 202 706-1 Environmental Engineering (EE); Measurement method for energy efficiency of wireless access network equipment; Part 1: Power consumption - static measurement method (Note: Annex E covers NR)
- [8] Hinton, K.J., Ayre, R., & Cheong, J. (2021). *Modeling the Power Consumption and Energy Efficiency of Telecommunications Networks* (1st ed.). CRC Press. <https://doi.org/10.1201/9780429287817>
- [9] S. C. Cripps, *RF Power Amplifiers for Wireless Communications*, 2nd ed. Artech House, 2006.
- [10] I. Seskar et al. O-RAN Energy Efficiency, O-RAN SuFG Meeting, Fukuoka, Japan, June 2025. [Online]. Available: <https://oranalliance.atlassian.net/wiki/download/attachments/40786665-73/2025-06-03>